

**Behavior of particles and gases in vehicle cabin**H. Jung<sup>1,2</sup><sup>1</sup>University of California, Riverside, <sup>2</sup>Emissions Analytics

The impact of air pollution on human health is a major concern and various anthropogenic sources of particulate exposure are under investigation to better understand their contributions to adverse health effects. Travel in vehicles represents a primary source of human exposure to particulate matter. A recent report estimated that for Los Angeles residents, 33-45% of exposure to ultrafine particles occurs while traveling in vehicles. Commuters on highways may be at particular risk, since particulate levels are demonstrably higher on highways. People living in urban areas are keen to reduce their exposure to particulate matter while riding a vehicle but there is a lack of information to make intelligent choices.

This study will show characteristic behavior of carbon monoxide, nitrogen oxides, ozone and particles in vehicle cabin in the presence of a passenger under various ventilation condition. This will give insight on how to control these pollutants in vehicle cabin.

The study will also definition a Cabin Air Quality Index (CAQI) to assess vehicle's ability to maintain clean cabin air quality similar to MPG for fuel economy. The study developed both static and dynamic test methods, which characterize and quantify vehicle cabin air quality from consumer's perspective.

The presentation will include details of the test method, results, and their implications. Standardization effort on CAQI via CEN workshop and VIAQ (Vehicle Interior Air Quality) IWG (Informal Working Group) under UNECE will be briefly explained at the end of the presentation.

## **Combustion-generated carbonaceous urban atmospheric UFPs: Efficiencies of face mask control of urban atmospheric particulate pollution: A pointer to control of future pandemics**

P. A. Sermon<sup>1</sup>, S. D. Rust<sup>1</sup>

<sup>1</sup>Laboratory for Nanoscale Materials, Bragg Building, CEDPS, Brunel University, Uxbridge, Middx., UB8 3PH, UK

Each day an adult human inhales on average 13.6kg [1] or 10,000 litres of air that potentially contains 0.1-10 trillion particles [2]. Some of these may be ultrafine carbonaceous combustion- and traffic-generated particles (UFPs) smaller than 100nm [3]. Others may be microbiological and bioaerosols (e.g. bacteria, fungi, viruses [4], excreta of insects and spores) and larger particulate (PM<sub>2.5</sub> or PM<sub>10</sub>) pollutants [3]. The corona COVID-19 virus is about 60-140nm [5,6]. Since we 'cannot cease breathing for more than a few minutes' [7] the atmosphere that bathes each of us is critical; locally this air is part of our personal ecosphere [8]. It has been suggested that pollution of urban air in London contributed to the death of Ella Kissi-Debrah in 2013. It is therefore worthy of assessing how filtration of critical atmospheric pollutants by face masks can be most beneficial. The ultrafine particles prevailing in the urban air in a covered carpark at UK postcode UB7 7GN were used to test the filtration efficiency of these masks using the P-Trak 8525.

Fine (100mmx100mm) and coarse (500mmx500mm) stainless steel filters had UFP filtration efficiencies of 50.87% and 7.29%. As one would expect, the bandana UFP filtration efficiency increased progressively from 45% to 90% as the number of bandana layers used to cover the face increased from 1 to 4. This is an important finding for control of current particulate air pollution and future pandemics. The UFP filtration efficiency of cycle and DIY masks was no better than a single layer bandana. The diodic valve KN95 mask was more than twice as efficient at filtering UFPs in an inhalation mode than in an exhalation mode, presumably protecting the wearer more than those around them.

Here the authors report which type of urban carbonaceous UFPs are filtered out and how this can be made selective with filter surface modification. The authors were also intrigued that passage through water stripped out carbonaceous UFPs from the atmosphere and this may affect the impact of the particles on our health and the modification of masks to protect us from these (and other) airborne hazards. Control of airborne infection and particulate pollutants is important as we protect personal ecospheres. Here we explore the varying respiration and retention of airborne carbonaceous UFPs by those of different gender, age group, fitness level and ethnic background so that they may be better protected in the future. For the moment, face masks show varying efficiencies for protecting us from inhaling combustion-generated airborne ultrafine particles (UFPs). Real-time technology to spot ineffective facemasks at their end-of-useful-life may need deploying. In addition, our understanding of the design of facemask filtering out carbonaceous UFPs will enable us to design even better masks for future pandemics.

**References:** [1] Anon Investigation of air pollution. Lancet Supplement i (27th Oct 1917); [2] Tsuda A. Particle transport and deposition: Basic physics of particle kinetics. Compr.Physiol. 3,1437-1471 (2013); [3] Kwon, H.S. Ultrafine particles: Unique physicochemical properties relevant to health and disease. Exoert.Molec.Med. DOI 10.1038/s12276-020-0405-1 (2020); [4] Milton D. K. Influenza virus aerosols in human exhaled breath: Particle size, culturability, and effect of surgical masks. Plos Pathogens 9,e1003205 (2013); [5] Leung, W. W-F. Charged PVDF multilayer nanofiber filter in filtering simulated airborne novel coronavirus (COVID-19) using ambient nano-aerosols. Sep.Purif.Technol. 245,116887 (2020); [6] Zhu, N. A novel coronavirus from patients with pneumonia in China, 2019. New Engl.J.Med. 737-731 (20th Feb 2020); [7] Giberne, A. The ocean of the air. Seeley, London (1894); [8] Garrett L. The coming plague p786



**Primary organic aerosol emissions and chemical composition from biomass and cow dung burning characterized using extractive electrospray ionization mass spectrometry**

J. Zhang<sup>1</sup>, K. Li<sup>1</sup>, T. Wang<sup>1</sup>, T. Cui<sup>1</sup>, L. Qi<sup>1</sup>, M. Surdu<sup>1</sup>, H. Lamkaddam<sup>1</sup>, I. El Haddad<sup>1</sup>, J. Slowik<sup>1</sup>, D. Bell<sup>1\*</sup>, A. Prevot<sup>1\*</sup>

<sup>1</sup>Laboratory of Atmospheric Chemistry, Paul Scherrer Institute, Villigen, 5232, Switzerland

Primary organic aerosol (POA) emitted from combustion processes (including biomass, waste and cow dung, etc...) may contribute a large fraction of organic aerosol (OA; including brown carbon (BrC)) on regional and global scale. POA from various sources has been closely linked to adverse health effects. However, comprehensive chemical characterization of POA emission is rarely reported due to its complexity and limitations of current instrumentation. The recently developed extractive electrospray ionization time-of-flight mass spectrometer (EESI-TOF) achieves real-time and near-molecular (i.e., molecular formula) measurement of water soluble constituents of POA<sup>[1]</sup>, which improves our understanding of the composition of POA. In this work, a series of experiments were conducted to investigate the emission factors (EFs), chemical composition, and marker ions of the POA from different combustion sources including wood, straw, and cow dung. The EFs of CO, CO<sub>2</sub>, non-methane hydrocarbon, and POA are 63.5±6.8, 1668.9±26.7, 10.4±2.7, and 3.7±1.1 g kg<sup>-1</sup> for wood open burning and 73.2±15.4, 1661.7±30.3, 11.7±2.9, and 1.7±0.4 g kg<sup>-1</sup> for wood stove burning, generally equivalent to straw burning (except for POA EF which is only 0.86 g kg<sup>-1</sup>) and lower than cow dung emissions. The carbon and oxygen distributions of POA vary between different burns and fuel types. Levoglucosan is the main marker for wood combustion, while its contribution to straw and cow dung burning is lower. In contrast, the total abundance of compounds with carbon number > 10 in the emission of straw and cow dung is higher than wood combustion. The proportion of nitrogen-containing compounds for cow dung burning is around 7%, which is higher than the proportion for wood and straw combustion with an average around 4%. The evaporation of main components of POA with temperature was analysed, providing insights into the volatility of POA and the effects of gas-particle partitioning on POA chemical composition.

We acknowledge the support of the SNF grant MOLORG (200020\_188624).

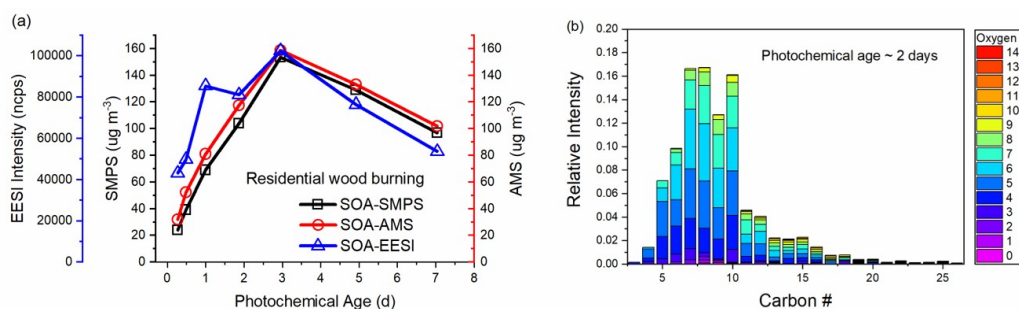
[1] Lopez-Hilfiker FD, et al. *Atmospheric Measurement Techniques*, 2019, 12, 4867-4886.

## Secondary nanoparticles formation and composition from open and residential wood burning

K. Li<sup>1</sup>, J. Zhang<sup>1</sup>, D. Bell<sup>1</sup>, T. Wang<sup>1</sup>, N. Hudda<sup>1</sup>, I. El Haddad<sup>1</sup>, J. Slowik<sup>1</sup>, A. Prevot<sup>1\*</sup>

<sup>1</sup>Laboratory of Atmospheric Chemistry, Paul Scherrer Institute

Biomass burning is one of the largest combustion-related sources of volatile organic compounds (VOCs) and nanoparticles to the atmosphere. However, the contribution of biomass burning to the regional and global secondary organic aerosol (SOA) burden is quite uncertain, limiting our understanding of its impacts on air quality, climate, and human health. One important issue related to the contribution estimating is the large uncertainty and variation of SOA yield and emission rate, especially the scarce data over long-timescale oxidation. Another issue is the lack of molecular composition and markers which can be used as references for ambient source apportionment. In this work, we studied the long-timescale oxidation of emissions from open and stove wood burning, representing wildfires and residential wood combustion, respectively. By deploying an extractive electrospray ionization time-of-flight mass spectrometer (EESI-TOF-MS) [1], we also provided the molecular-level chemical composition of the formed SOA. The results of this work can largely improve our understanding of the contribution of biomass burning to the SOA burden. **Methods.** Pine and spruce wood were burned open or in a residential stove, and the burning emissions were injected into a holding chamber. Photooxidation experiments were conducted using a custom-made oxidation flow reactor (OFR) [2]. The burning emissions were introduced into the OFR from the holding chamber with a small flow. Particle size distribution was measured with a scanning mobility particle sizer (SMPS, TSI), and was used to determine the SOA mass concentration. Bulk composition and oxidation state of particles were determined using a long time-of-flight aerosol mass spectrometer (LTOF-AMS, Aerodyne). The molecular composition of particles was measured with an EESI-TOF-MS [1]. **Results.** SOA mass concentration measured by SMPS and AMS matches very well. Although EESI data has some variations, the general trend in the SOA concentration is very similar: it firstly increases and then decreases with increasing photochemical age. This indicates that fragmentation reactions might play an important role, which can be proved by the decreasing average carbon number (from 10 to 8) measured by EESI with increasing photochemical age (from 0.3 to 7 days). In addition, it is found that there is no significant difference in SOA production from open or stove burning emissions. The carbon and oxygen distributions of the formed SOA show that the majority of SOA are species with carbon number  $\leq 12$  and oxygen number  $\leq 7$ . The time evolution of these species provides insights into the chemistry in the oxidation of biomass burning emissions.



[1] Lopez-Hilfiker, F. D. et al., *Atmos. Meas. Tech.*, **2019**, 12, 4867-4886.

[2] Li, K. et al., *Atmos. Chem. Phys.*, **2019**, 19, 9715-9731.

**Network analysis for the formation of aromatics in a co-flow flame**A. Violi<sup>1</sup><sup>1</sup>University of Michigan

An important step in predicting the growth of soot nanoparticles is understanding how gas phase variations affect the formation of their aromatic precursors. Once formed, these aromatic structures begin to assemble into nanoparticles and, regardless of the clustering process, the molecular properties of the aromatic precursors play an important role.

In this work, we report on a detailed study of the spatial evolution of molecular structures of polycyclic aromatic compounds (PACs) and their corresponding formation pathways. To this end, we employed the SNapS2 kinetic Monte Carlo software to simulate the chemical evolution of PACs along multiple streamlines. The results show that growth only occurs along streamlines that traverse regions of high acetylene concentrations in the center of the flame. The PACs predicted in various conditions show diverse chemical properties, including aliphatic chains, five-membered, and heteroaromatic rings. PACs in streamlines close to the flame wings begin growing immediately due to the high temperature and large amounts of radical species, while PACs originating along inner streamlines do not appreciably grow until they pass through an area characterized by high radical concentrations. Using graph theory and network analysis, we investigated the complex reaction network generated by SNapS2 and determined that the growth pathways of many PACs center around a few stable structures that also promote oxygen addition reactions due to their morphology and long lifetimes.

These pathways play a significant role along streamlines near the centerline, compared to the flame wings, which show more variety due to the highly reactive environment encountered during early growth. The results of this study provide insights on the reaction pathways that determine the properties of PACs at different flame locations as well as information on the chemical characteristics of the formed PACs, with emphasis on oxygenated structures.

## Study of soot production in ethylene pyrolysis using a sectional model

L. Pachano<sup>1</sup>, D. Aubagnac-Karkar<sup>1</sup>

<sup>1</sup>IFP Energies nouvelles, 1-4 avenue de Bois-Préau, 92852 Rueil-Malmaison, France

The interest in studying nanoparticle formation from hydrocarbons oxidation and pyrolysis is twofold. On one hand, it is crucial for suppressing undesirable soot emissions that might impact the environment and human health. On the other hand, it is of interest for the developing of more efficient processes for nanoparticle synthesis. Within this context, this work aims at modeling soot production in ethylene pyrolysis using a sectional approach. To that end, the main focus is placed on the assessment of results sensitivity to the gas-phase mechanism, soot precursors and surface growth mechanism.

The consecution of the objective relies on the validation of polycyclic aromatic hydrocarbons (PAH) and major species concentration along with soot predictions. For this validation, two experimental datasets are targeted. The first dataset comprises measurements from experiments conducted in a plug flow reactor (PFR) at atmospheric pressure and low temperature (1223-1423 K) [1]. The second dataset includes time-resolved profiles from the pyrolysis of ethylene in a shock tube (ST) at high pressure (around 0.38 MPa) and high temperature (1961-2179 K) [2]. Cantera is used to solve the chemical kinetics from several gas-phase mechanisms describing ethylene pyrolysis. Implemented within the framework of Cantera, a soot sectional model (SSM) [3] is used to account for soot production. The SSM considers soot particles to be a solid and distinct dispersed phase interacting with the gas-phase through a two-way coupling.

Modeling results evidence large differences in the prediction of PAH mole fraction for the different gas-phase mechanisms evaluated for the PFR cases. These differences, in addition to the choice of soot precursors, are shown to heavily influence soot predictions. Time-resolved soot volume fraction profiles, from the ST cases, allow assessing how the soot onset time is influenced by the soot precursors choice. In relation to the sensitivity of results to the soot surface growth mechanism, both PFR and ST results point out to the importance of the carbon balance between the soot and the gas-phase to the accurate prediction of soot production. In that sense, PFR cases show a clear over-prediction of acetylene mole fraction if soot production is not accounted for.

[1] N. E. Sánchez, A. Callejas, Á. Millera, R. Bilbao, M. U. Alzueta, *Energy Fuels* **2012**, *26* (8), 4823–4829. DOI: 10.1021/ef300749q.

[2] U. KC, M. Beshir, A. Farooq, *Proceedings of the Combustion Institute* **2017**, *36* (1), 833–840. DOI: 10.1016/j.proci.2016.08.087.

[3] D. Aubagnac-Karkar, A. El Bakali, P. Desgroux, *Combustion and Flame* **2018**, *189*, 190–206. DOI: 10.1016/j.combustflame.2017.10.027.

**Impact of organic carbon on soot light absorption**G. A. Kelesidis<sup>1</sup>, C. A. Bruun<sup>1</sup>, S. E. Pratsinis<sup>1\*</sup><sup>1</sup>ETH Zurich

Carbonaceous nanoparticles (e.g., soot, carbon black and quantum dots), nanotubes and graphene are produced by fuel-rich combustion in aerosol and biomass reactors. The light absorption of these nanoparticles is essential for their characterization by laser induced incandescence and light extinction [1]. For example, carbon black and graphene absorb strongly light due to their similar composition of sp<sup>2</sup>-bonded aromatics. In contrast, the optical properties of soot may differ significantly from those of carbon black and graphene [10]. This is due to the fact that light absorption of soot depends on its C/H, maturity [2], morphology [3] and organic carbon (OC) content [4]. Here, the impact of OC on the light absorption of soot is determined by discrete element modeling coupled with the discrete dipole approximation for computing the scattering of radiation by soot particles. The mass absorption cross-section (*MAC*) of soot is used widely to determine its light absorption. Typically *MAC* is obtained from the mass average refractive index of OC and elemental carbon (EC) with large C/H that make up mature soot. As such, *MAC* can be overestimated by a factor of 3 in fuel-rich flames where newly-formed young soot contains EC with small C/H and OC that predominantly scatters light reducing its absorption by soot. Here a relation for the soot refractive index is derived accounting for soot morphology, maturity and OC content through its band gap at wavelength,  $\lambda = 266 - 1064$  nm. Using this relation, the *MAC* of soot containing OC (up to 50 wt%) is in excellent agreement with carbon black, graphene and soot data at  $\lambda = 300 - 840$  nm. This confirms that soot morphology, maturity and OC content greatly influence light absorption during characterization of in-flame and freshly-emitted soot by laser induced incandescence and light extinction, especially in fuel-rich flames, and need to be properly accounted for in the soot refractive index.

[1] Georgios A. Kelesidis, Sotiris E. Pratsinis, *Proceedings of the Combustion Institute*, in press: doi.org/10.1016/j.proci.2020.07.055.

[2] Georgios A. Kelesidis, Sotiris E. Pratsinis, *Proceedings of the Combustion Institute*, **2019**, 37, 1177-1184.

[3] Georgios A. Kelesidis, M. Reza Kholghy, Joel Zurcher, Julian Robertz, Martin Allemann, Aleksandar Duric, Sotiris E. Pratsinis, *Powder Technology*, **2020**, 365, 52-59.

[4] Georgios A. Kelesidis, Christian A. Bruun, Sotiris E. Pratsinis, *Carbon*, **2021**, 172, 742-749.

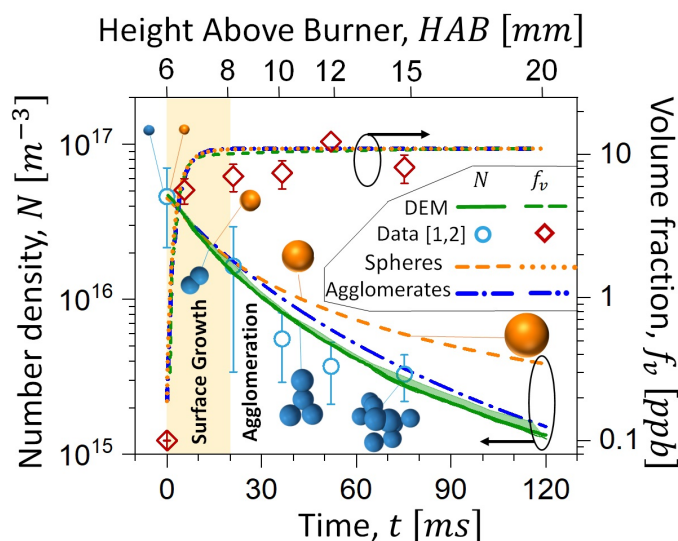


## Surface growth, coagulation and oxidation of soot by a monodisperse population balance model

R. Kholghy<sup>1</sup>

<sup>1</sup>Carleton University

A monodisperse population balance model (MPBM) is developed here that capitalizes on the rapid attainment of the self-preserving size distribution and asymptotic fractal-like structure of agglomerates by coagulation to simulate their evolution with only three equations. Total agglomerate carbon molar,  $C$ , number ( $N$ ) and area ( $A$ ) concentrations are tracked. The model accounts for the polydispersity of agglomerates by enhancing their collision frequency by that of their self-preserving size distribution based on the radius of gyration in the free molecular regime. Scaling laws from detailed discrete element modeling (DEM) simulations are used to describe the fractal-like morphology of the agglomerates. The MPBM predicts the evolution of soot  $f_v$ ,  $N$  and average mobility and primary particle diameters during surface growth and agglomeration in laminar premixed ethylene flames as well as soot oxidation in a tube reactor within 30% of detailed DEM, sectional population balance simulations and measurements. Thus, when self-preserving size distribution and asymptotic structure of agglomerates are attained, this simple MPBM has unprecedented accuracy and can be readily interfaced with computational fluid dynamic (CFD) to model soot formation in combustion devices or process design and optimization for the synthesis of carbonaceous agglomerate nanoparticles.



Evolution of soot volume fraction,  $f_v$  (dashed green line) and number density,  $N$  (solid green line) during agglomeration and surface growth.

[1] A.D. Abid, N. Heinz, E.D. Tolmachoff, D.J. Phares, C.S. Campbell, H. Wang, *Combust. Flame*, 154 (2008), 775.

[2] J. Camacho, C. Liu, C. Gu, H. Lin, Z. Huang, Q. Tang, X. You, C. Saggese, Y. Li, H. Jung, *Combust. Flame*, 162 (2015), 3810.

## Particle number emissions from a Euro 6d-temp GDI under extreme European temperature and driving conditions

J. Andersson<sup>1</sup>, B. Giechaskiel<sup>2</sup>, A. Kontses<sup>3</sup>, A. Balazs<sup>4</sup>, Z. Samaras<sup>3</sup>

<sup>1</sup>Ricardo Automotive and Industrial, Shoreham-by-Sea, UK, <sup>2</sup>JRC, Ispra, Italy, <sup>3</sup>LAT, Thessaloniki, Greece, <sup>4</sup>FEV, Aachen, Germany

With the introduction of gasoline particulate filters (GPFs) the particle number (PN) emissions of gasoline direct injection (GDI) vehicles are below the European regulatory limit of  $6 \times 10^{11}$  p/km under certification conditions. Nevertheless, when considering more robust legislation for light-duty vehicles at Euro 7, concerns have been raised regarding the emission levels at the boundaries of ambient and driving conditions of the real-driving emissions (RDE) regulation. A Euro 6d-Temp GDI vehicle with GPF was tested on the road and in the laboratory with cycles simulating urban congested traffic, dynamic driving, and uphill driving towing a trailer at 85% of the maximum payload. The ambient temperatures covered a range from  $-30^{\circ}\text{C}$  up to  $+50^{\circ}\text{C}$ . The solid PN emissions were ten times lower than the current PN limit under most conditions and temperatures. Only dynamic driving that passively regenerated the filter, and the cycle after, resulted in relatively high emissions, but still below the limit. The results of this study confirm the effectiveness of GPFs in controlling PN emissions under a wide range of conditions. Related analysis of late Euro 6 diesel vehicles indicates continued effectiveness of DPFs irrespective of boundary conditions. Potential limit values, proposed by the CLOVE Consortium, for PN emissions of light-duty vehicles at Euro 7 will be presented.